MONTE CARLO SIMULATIONS OF ELECTRON LATERAL DISTRIBUTIONS IN THE CORE REGION OF 10^{13} - 10^{16} eV AIR SHOWERS

A.G. Ash

Department of Physics
University of Leeds
Leeds LS2 9JT
U.K.

ABSTRACT

This paper contains details of computer models of shower development which have been used to investigate the experimental data on shower cores observed in the Leeds $35m^2$ and Sacramento Peak (New Mexico) $20m^2$ arrays of current-limited spark ("discharge") chambers. The simulations include predictions for primaries ranging from protons to iron nuclei (with heavy nuclei treated using both superposition and fragmentation models).

1. Introduction

Analysis of photographs of 10^{14} - 10^{16} eV air shower cores in arrays of current-limited spark chambers at Leeds (1020 g cm^{-2}) and Sacramento Peak (730 g cm^{-2}) has provided data on particle distributions within a few metres of the shower axis in the form of density spectra and density averages measured at known fixed distances from the shower centre (Ash, 1985a, Hodson et al., 1983a,b, 1985). Comparison of these results with Monte Carlo simulation predictions by Ash (1985a,b) has demonstrated the failure of the scaling model. Details of the calculations are presented in this paper (see also Ash, 1984).

2. Hadron collision models

Simulation techniques based in the laboratory frame were used, and the models generated only pions and leading nucleons; nuclear target effects were neglected. The energy-splitting algorithms of Hillas (1981) were used to generate "radial scaling" secondary energy spectra in pion collisions (Fig.1a) and nucleon collisions (Fig.1b), except that for the latter, the flat leading nucleon spectrum given was replaced by a more accurate form (Hillas, 1979a): the elasticity $X = E_{nuc}/E_o$ was sampled using $X = 0{\cdot}76a + 0{\cdot}24a^4$ (instead of $X = a$) where a is a random number ($0{\cdot}0....1{\cdot}0$). (If, as a result, E_{nuc} was less than the nucleon rest energy mc^2 then $E_{nuc} = mc^2$). For $E_o \gg mc^2$ the resulting average elasticity is equal to 0·42.

Transverse momenta were sampled from the energy-independent distribution $h(p_t)dp_t \propto p_t e^{-p_t/p_o}$ with p_o equal to 0·24 GeV/c for secondary pions (in both pion and nucleon collisions) and equal to 0·28 GeV/c for leading nucleons. (If $p_t \geq p$ then the secondary was considered to be going backwards and was dropped from the cascade.)

Mean free paths for nucleon-'air' nucleus collisions (Fig.2) based on nucleon-nucleon cross sections rising as $\ell n^2 s$ at high energy were as

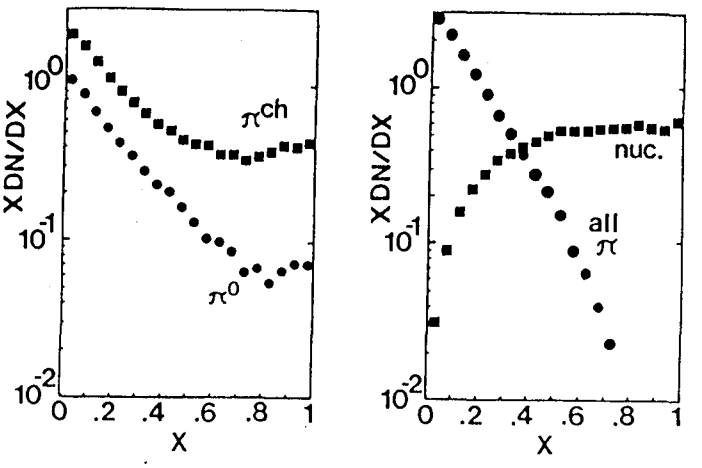

(a) Pion collisions (b) Nucleon collisions

Fig. 1 Particle production spectra in simulated 100 GeV hadron-'air' nucleus collisions. X is the secondary energy divided by the projectile energy, both measured in the laboratory frame

given by Hillas (1979b); those for pion collisions were obtained by scaling up the nucleon mean free paths by (114/86) at all energies.

3. Nuclear fragmentation models

The "superposition model" was used i.e. a shower with primary mass number A, energy E_{prim}, was taken as a co-axial superposition of A proton showers with energy E_{prim}/A. A more realistic treatment of primaries ranging from helium nuclei to iron nuclei was given in the one-dimensional "fragmentation model" which is based mainly on emulsion data and follows quite closely the Bartol model (Gaisser et al., 1982) with which it is in good agreement for the average distribution in the atmosphere of the "first" inelastic collisions of primary nucleons. Excellent agreement with Freier and Waddington's (1975) simulation predictions of the average rate of release of nucleons from projectile nuclei as a function of atmospheric depth is obtained using the Cleghorn nucleus-nucleus cross sections, adopted by them, instead of the larger cross-sections of Gaisser et al. (1982) normally used.

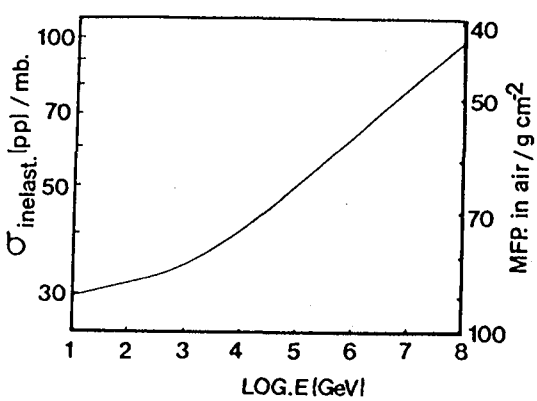

Fig. 2 Inelastic pp cross-sections and corresponding mean-free-paths in air used in simulations

4. Propagation model

A non-isothermal atmosphere was used. Coulomb scattering and ionisation loss (2·2 MeV per g cm^{-2}) were applied to hadrons, but were neglected for projectile nuclei in the "fragmentation model". Geomagnetic effects were neglected.

5. Electromagnetic cascade function

An average development function based on unpublished Monte Carlo calculations for photon-initiated cascades by A.M. Hillas was used. The electron density at 1020 g cm^{-2} (Leeds) for cascades due to vertical photons was

$$\rho(r) = \frac{1}{2\pi r}\frac{dn(r)}{dr}(1 + r/45)^{-3} \quad m^{-2} \quad \text{with} \quad n(r) = \frac{a}{\sqrt{y}} e^{t(1 + \ln f/0{\cdot}72)}$$

$$\text{and} \quad a = 0{\cdot}460/(1 + 0{\cdot}380/x) \qquad x = E.r/5{\cdot}8093$$

$$f = 1 - 0{\cdot}72(1 - y/t) \qquad y = \ln(1 + 2{\cdot}390x)$$

E is the photon energy in GeV, and t is the vertical thickness (r.l.) between the photon production point (π^0 decay) and the observation level. A radiation length of 36·1 g cm^{-2} was used. If a cascade was inclined this was taken into account by multiplying the density calculated from the formula by the cosine of the zenith angle and taking t equal to the slant thickness, and r equal to the perpendicular distance from the cascade axis.

The cascade function has been used directly for each photon (EMC Model I) or in conjunction with a simple Monte Carlo technique to simulate fluctuations in the formation of the first e^+e^- pair (EMC Model II).

Mountain level calculations involved rescaling the above electromagnetic cascade lateral distributions according to the lower air density.

6. Simulation of the electron distribution in the shower core

(a) Calculations for Leeds

A map of the core region was obtained by superposing electromagnetic cascades, taking into account the direction and location of their axes. In each shower simulation the shower primary was directed at the centre of a square of side 10·2 m located in the observation plane. The square was subdivided into $(51)^2$ equal squares, and the counts of electrons deposited in each of them determined using the cascade function. Computing time consumed in doing this was saved by ranking photons so as to concentrate the most detailed calculations on photon cascades with the densest "cores", and by "thin sampling" (Hillas, 1981) of low energy hadrons. Calculations for photon energies down to 1 GeV from π^0 decay could therefore be made on a routine basis.

After calculating the electron counts the simulation program searched for a shower centre (centre of symmetry) in the central $(7{\cdot}6)^2$ m^2 of the mapping area (most of the shower centres, located to within $\sim$5cm, fall within 0.5 m of the centre of the mapping area). The shower was discarded if a shower centre was not found in the "search area", and also if the electron density, averaged over 2 × 2 adjacent square elements of the mapping area, did not exceed 50 m^{-2} somewhere in the mapping area.

If the shower was not discarded then densities at various radial distances from the shower centre were obtained, as in the experimental work (Hodson et al., 1983a,b, 1985), from counts made in an "annular

grid", in this case, "superposed" over the mapping area. The grid used consisted, as in the experiment, of a series of concentric circles, starting with a radius of 0·25 m and then with radii increasing in 0·5 m steps. For the above experimental work the annuli were divided into equal areas of $\pi/16 m^2$. However for the simulations it was more convenient to divide the annuli angularly each into 16 sections ("sampling bins") by common radii from the centre. The difference between the two procedures is not significant: both give densities for the same radial widths.

Counts were obtained in the "sampling bins" with the "annular grid" centred on the shower centre. The central count, calculated by integrating the electron density over the area of the central bin, gave the density corresponding to the experimental central density $\rho(0)$. Counts in the annuli at 1·0, 2·5 and 4·0 m were derived from the mapping area counts and gave densities corresponding to the experimental densities $\rho(1·0)$, $\rho(2·5)$ and $\rho(4·0)$ respectively. These results were supplemented by counts, determined as above, in the remaining annuli out to 4·5 m and by densities calculated at points in the mapping plane further out. The radial density distribution was thus sampled at intervals of 0·5 m out to 7·0 m from the shower centre.

(b) Calculations for Sacramento Peak

Both the calculations and the experimental analysis are made using the corresponding Leeds-level grids with dimensions in array space scaled up according to the lower air density found at mountain level.

7. Construction of density spectra etc.

Predictions of the average lateral distribution and density spectra at fixed distances from the shower centre have been obtained for a wide choice of primary composition and energy spectra. A technique of weighting the simulated showers according to the primary fluxes assumed was used to obtain results for different primary energy spectra.

8. Acknowledgements

The author thanks Dr A.M. Hillas for his help with this work, and the Science and Engineering Research Council for support in the form of a Post-Doctoral Research Fellowship.

References

Ash, A.G., 1984, Ph.D.thesis, University of Leeds
Ash, A.G., 1985a, paper HE4.2-18, this Conference
Ash, A.G., 1985b, paper HE4.2-16, this Conference
Freier, P.S. and Waddington, C.J., 1975, Astrophys.Sp.Sci., 38, 419
Gaisser, T.K. et al., 1982, Phys.Rev., D25, 2341
Hillas, A.M., 1979a, Haverah Park Note, September 1979
Hillas, A.M., 1979b, 16th ICRC, Kyoto, 6, 13
Hillas, A.M., 1981, 17th ICRC, Paris, 8, 193
Hodson, A.L. et al., 1983a, 18th ICRC, Bangalore, 6, 23
Hodson, A.L. et al., 1983b, 18th ICRC, Bangalore, 11, 201
Hodson, A.L. et al., 1985, paper HE4.2-10, this Conference